**Proceedings of IMECE2006**
**2006 ASME International Mechanical Engineering Congress and Exposition**
**November 5-10, 2006, Chicago, Illinois, USA**

# IMECE2006-13223

# DEFORMATION EFFECTS ON THE LOAD CARRYING CAPACITY OF THE BARREL BEARING IN AXIAL PISTON PUMPS AND MOTORS

Peter A.J. Achten/Innas BV

Marc P.A. Schellekens/Innas BV

## ABSTRACT

Most hydrostatic pumps and motors apply mechanical face seals, often also acting as a thrust bearing. The load carrying capacity of these bearings is very much dependent on the pressure profile generated in the sealing gap. Previous research, outside pumps and motors, has already shown that the gap pressure profile is largely influenced by small radial deformations of the seal lands. This paper discusses the elastic deformation of pump components and the effects of these deformations on the load carrying capacity of a barrel in an axial piston machine.

## NOMENCLATURE

| | |
|---|---|
| $A$ | Area |
| $b$ | width leakage path |
| $def$ | deformation |
| $F$ | force |
| $h$ | gap height |
| $\Delta h$ | gap height variation |
| $L$ | length leakage path |
| $M$ | torque |
| $\Delta M$ | torque loss |
| $n$ | rotational speed |
| $p$ | pressure |
| $Q$ | leakage flow |
| $R$ | resistance coefficient |
| $r$ | radius |
| $V$ | displacement volume |
| $x$ | coordinate |
| $y$ | coordinate |
| $z$ | coordinate |

Greek symbols:

| | |
|---|---|
| $\beta$ | angle between barrel and rotor |
| $\mu$ | coulomb friction coefficient |
| $\eta$ | dynamic viscosity |
| $\lambda$ | taper ratio |
| $\varphi$ | rotational coordinate |

Subscripts:

| | |
|---|---|
| $e$ | end of the leakage gap |
| $s$ | start of the leakage gap |
| $par$ | parallel gap profile |
| $tap$ | tapered gap profile |
| $sp$ | spring |
| $cyl$ | cylinder |
| $vf$ | viscous friction |
| $bf$ | barrel friction |
| $cf$ | coulomb friction |

## THE ANGEL IS IN THE DETAIL

Some machines just work. We don't know why or how but they do. An axial piston pump or motor can be considered as such a machine. Although the general principle is obvious and beyond any dispute, the hydrostatic thrust bearings applied in these machines are far from self-explanatory. Axial piston pumps (Figure 1), as well as most other hydrostatic pumps, have a number of these bearings that also operate as a mechanical face seal: the bearings have to carry a load and simultaneously seal of a leakage path. This implies that the existence of an oil film between the moving and the stationary part is necessary in order to prevent metal-to-metal contact and avoid excessive wear, friction losses and (local) heat generation. On the other hand the thickness of the oil film is only allowed to be a few micrometers, otherwise leakage losses would strongly increase.

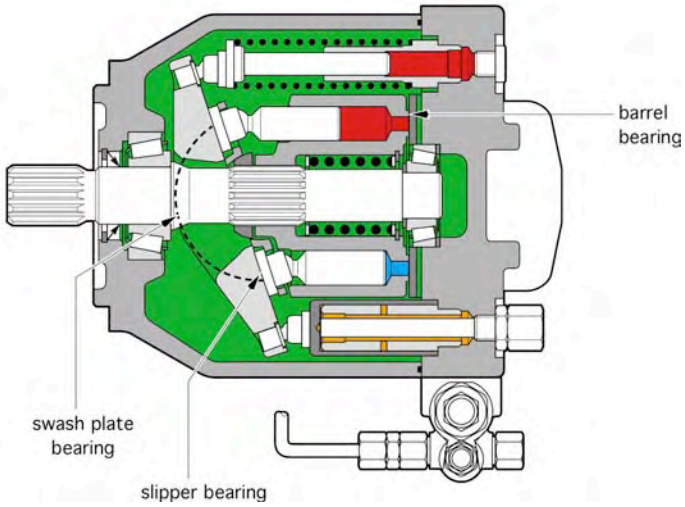


**Fig. 1: hydrostatic bearings in an axial piston slipper type pump**

But what principle makes a slipper or a barrel run on the surface of its stationary counterpart at a distance of only a few micrometers? Fundamental research in the field of the tribology of thrust bearings and face seals [1…8] has revealed that elastic deformation of the components causes a gap which is not parallel in the direction of the leakage path. In 1991 Lebeck [1] concluded: "Deviations from parallelism (tilt, taper, or waviness) cause a strong hydrodynamic or hydrostatic load support. Geometry factors that cause such deviations from parallel, either by accident or by design, should be given primary consideration in developing models of seal behavior." In the area of hydrostatic pumps and motors Yamaguchi was one of the first to investigate the effect of elastohydrodynamic (EHD) deformation on the load carrying capacity of hydrostatic bearings [1…3]. Recently also Manring, Winkler, Huang and Ivantysynova [12…18] included EHD-effects in their models and investigations.

According to Manring "small bearing deformations have a significant impact on the pressure profile that is generated between the bearing and the thrust surface" [15]. This corresponds with the earlier conclusions of Lebeck. There are however some major differences between general thrust bearings and thrust bearings applied in hydrostatic pumps and motors. Outside pumps and motors, the heat generated in face seals and thrust bearings often results in a significant temperature increase of the bearing components. The resulting thermal expansion of these components causes a tapered gap, which can increase or decrease the load carrying capacity, depending whether the bearing deforms convex or concave.

In hydrostatic pumps and motors, thermal effects will be much more limited due to the oil flow acting as a coolant. The pressure levels are however much higher and consequently it is to be expected that the hydrostatic loads will have a much larger influence on the deformation of the mechanical components. Moreover the gap heights have to be smaller for compensating the larger pressure difference across the sealing gap. As a result the ratio between the deformation and the average gap height will increase, making the construction more sensitive for deformation effects.

This paper describes the influence of the deformation on the load carrying capacity of the barrel and other thrust bearings in hydrostatic pumps and motors. As will be shown the pressure load acting on the lands of the face seals cause the gap between the bearing and its thrust to become tapered in the direction of the leakage flow. The tapered shape creates a change of the pressure profile and consequently changes the load carrying capacity of the oil film. The extra lifting force is not constant but becomes smaller when the barrel is lifted from the port plate. In the end, assuming a converging gap profile, the barrel is lifted just a few micrometers from the port plate where it finds a stable position.

## FEM ANALYSIS OF BARREL, VALVE PLATE AND COVER

In order to study the effects of the pressure load on the hydrostatic deformation of seal lands in a hydrostatic pump, a detailed final element analysis of the main components is needed. Several researchers have reported about FEM-analyses of axial piston pumps and their components [19…22]. In most cases the analysis was performed to study the vibration modes of a pump or a motor. This publication focuses specifically on the deformation of the components that influence the face seal between the barrel and its port plate.

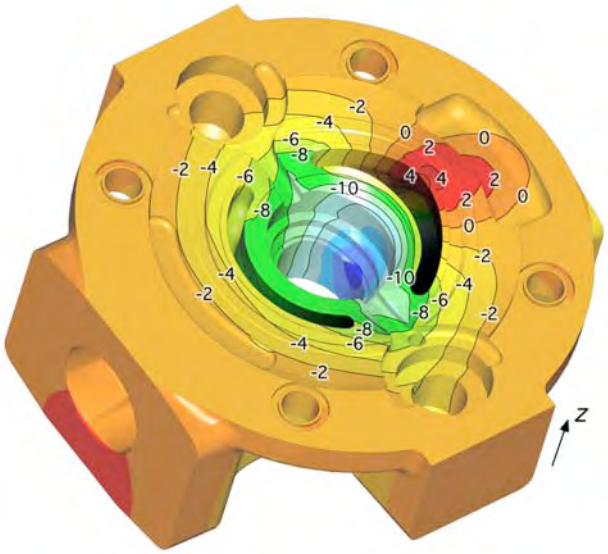


**Fig. 2: Axial deformation in the *z*-direction (in µm) of a cover block of a slipper type pump at a pump pressure of 35 MPa.**

The finite element analysis presented in this paragraph is about an assembly of three components of a 45 cc/rev slipper type pump: the steel barrel, the brass port plate and the cast iron cover of the housing. Figure 2 shows the deformation in the axial *z*-direction of the cover of the pump at a pump pressure of 35 MPa. The high-pressure port is at the right side. The largest deformation is at inner seal land where the hydrostatic pressure acting on the housing is not compensated by another pressure

field. Opposed to this, at the outer seal land, the pressurized output channel pushes the material back in the upward direction, thereby creating a significant protrusion in the deformation landscape.

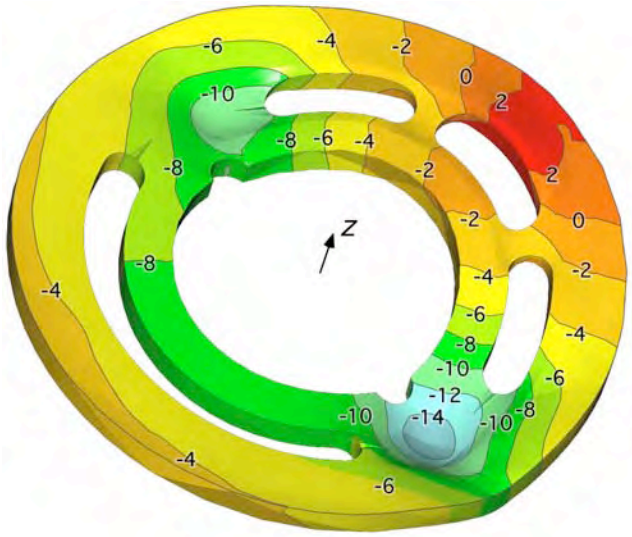


**Fig. 3: Axial deformation in µm of the port plate (*p* = 35 MPa)**

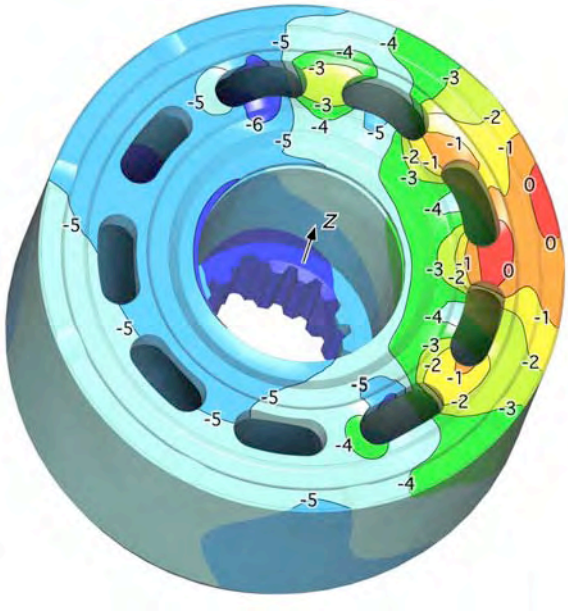


**Fig. 4: Axial deformation of the barrel in µm (*p* = 35 MPa)**

The port plate (Figure 3) on top of the cover follows to some extent the axial *z*-deformation of the cover block. As before, the right side of the port plate is pressurized. The calculation is performed at a barrel position at which a pressurized barrel port is standing exactly between the high-pressure and low-pressure kidney of the valve plate. At this position, the backside of the port plate does not have a corresponding pressure field and is not supported by the housing. As a result, the port plate is pushed down at this location creating a substantial valley in the deformation landscape. At the opposite site of the port plate, only half a barrel port is at the sealing land, and the deformation is less severe. Furthermore, due to the locale deformation of the supporting cover block, the port plate also has a bump at about the middle of the high-pressure kidney.

In order to obtain information about the gap height between the barrel and the port plate the deformation of the barrel it self has to be calculated as well. Figure 4 gives the results of the FEM-analysis. As before, only the deformation in the *z*-direction is shown. Compared to the housing, the barrel deformation is smaller due to the stiffer construction. Even so, the deformation of the seal lands in the *z*-direction is up to 6 µm.

For further investigation of the deformation effects on the local gap height between the barrel and the port plate, 8 circular curves are defined (see Figure 5): 4 on the barrel and 4 corresponding curves on the port plate. The curves are numbered from the inside out. The first, inner two curves are at the end and the beginning of the inner seal land. The other two curves are at the beginning and end of the outer seal land. The rotational coordinate $\varphi$ is defined in Figure 5 and starts in the middle of the low-pressure kidney. Since we want to calculate the gap height we are again only interested in the deformation in the axial *z*-direction.

Figure 6 shows the deformation curves for the inner seal land (Figure 6a) and the outer seal land (Figure 6b). The high-pressure zone indicated by the grayed area in these plots reflects the five out of nine cylinders that are connected to the high-pressure kidney of the port plate.

The gap heights can now easily be calculated by subtracting the deformation of the port plate from the deformation of the barrel. The results are shown in Figure 7, for the inner seal land (curves $h_1$ and $h_2$) as well as for the outer seal land ($h_3$ and $h_4$). The deformation is calculated assuming a contact establishes between the barrel and the port plate: the Herz contact pressures of the contact areas counteract the remaining force of the barrel pushing to the port plate. According to the FEM-analysis the contact is established at the low-pressure side at the outer support ring of the barrel, and about at the middle of the high-pressure kidney (see the curve of $h_4$ in Figure 7b).

The curves of figures 6 and 7 show the large variation of the gap height, having the largest gap around the top and bottom dead centre positions ($\varphi$ = -90° and $\varphi$ = 90°) where the cover block of the housing does not support the port plate sufficiently. The calculated gap height is almost zero at the middle of the high-pressure kidney ($\varphi$ = 0°) where the protrusion of the housing bents the port plate upwards.

Aside from the variation of the gap height in the $\varphi$-direction there is also a much smaller variation of the gap height in the radial direction. Figure 8 plots the variation of the gap height, subtracting the gap height at the end of the leakage path from the gap height at the beginning of the leakage path:

$$\Delta h = h_e - h_s \quad \left(\Delta h \geq -h_s\right) \tag{1}$$

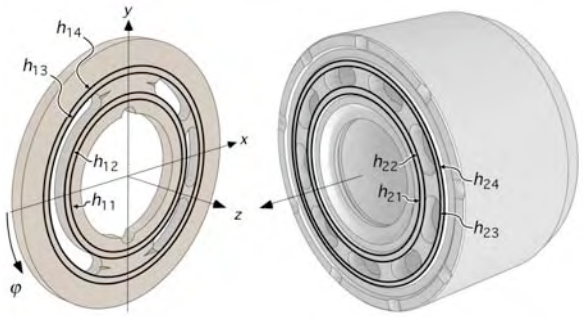


**Fig. 5: Seal land curve definitions of port plate and barrel.**

6a..

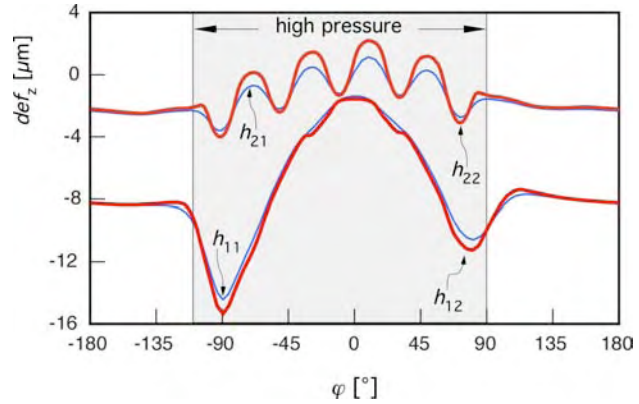


6b.

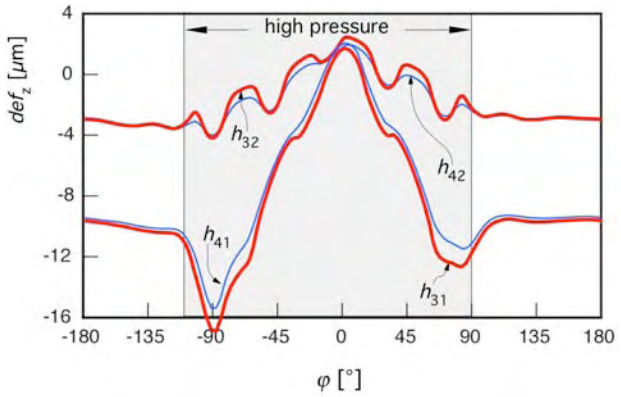


**Fig. 6: Axial deformation of the barrel and the port plate (6a: inner seal land, 6b: outer seal land)**

7a..

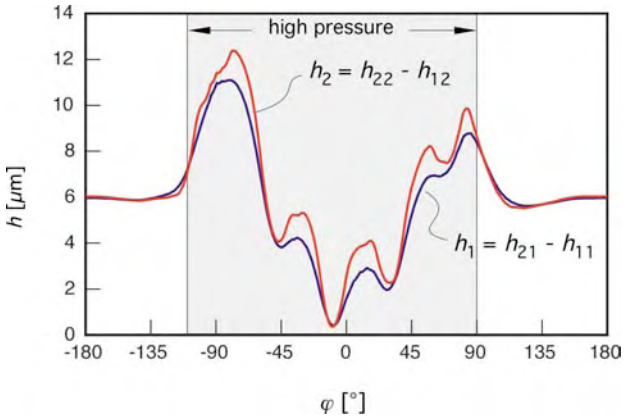


7b.

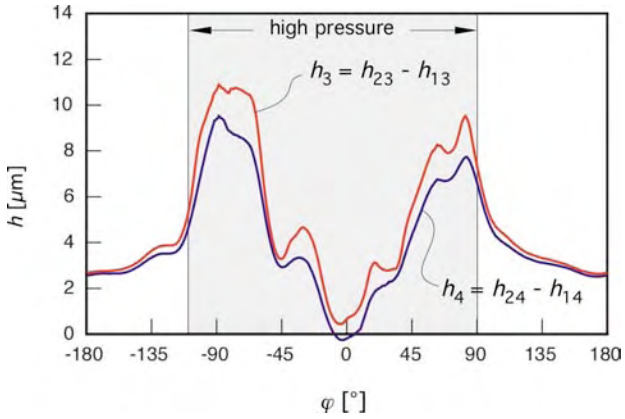


**Fig. 7: Calculated gap heights (6a: inner seal land, 6b: outer seal land)**

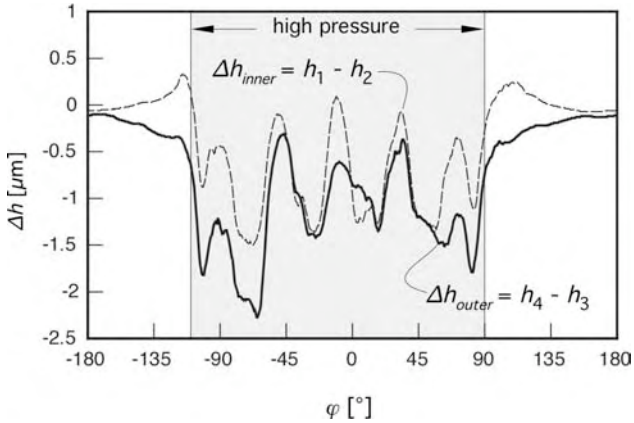


**Fig. 8: Variation of the gap height across the leakage gap**

Almost over the entire range, and especially in the high-pressure zone, the change of gap height $\Delta h$ across the leakage flow path has a negative value. This shows that the gap height is larger at the beginning of the leakage path than at the end. Consequently the gap has a converging, tapered shape (see Figure 9). In the high-pressure zone, the tapered effect is caused by the general deformation as well as by the local pressure profile in the gap, having a high pressure at the start of the leakage path and the low, internal pressure of the housing at the end of the gap.

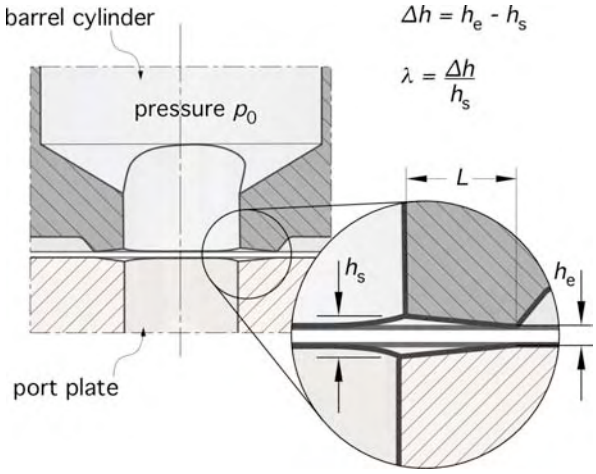


**Fig. 9: Local deformation of the seal lands of the barrel and the port plate**

At the low pressure side the inner seal land has a divergent gap height ($\Delta h > 0$) and a convergent gap ($\Delta h < 0$) at the outer seal land. Here the tapered gap profile is not generated by the pressure in the gap but only by the general deformation and tilted position of the barrel.

## RADIAL TAPER EFFECTS

The tapered shape of the leakage gap has a significant effect on the hydrostatic balance of the barrel bearing as well as on the leakage flow. In order to obtain a better understanding of this effect, a simple straight gap is defined with a length $L$ of the leakage path and a gap width $b$. The gap profile (see Figure 9) is assumed to vary linearly, having a height $h_s$ at the start, and $h_e$ at the end of the flow path:

$$\begin{aligned} h(x) &= (h_e - h_s)\cdot\frac{x}{L} + h_s \\ &= \Delta h\cdot\frac{x}{L} + h_s \end{aligned} \tag{2}$$

In this equation $x$ is the local position in the gap, following the leakage path.

The oil flow through the gap is assumed to be laminar and isoviscous (see Appendix A). Furthermore fluid inertia effects and effects of surface roughness on the fluid flow are assumed to be negligible. The gap itself is supposed to be uniform across its width and the gap geometry does not to change over time, hence buffer effects do not have to be taken into account.

Assuming a zero pressure in the housing, the leakage flow through the gap can be calculated by means of the general laminar flow equation:

$$Q = \frac{1}{R}\frac{p_0}{12\eta}b \tag{3}$$

with $p_0$ being the pump pressure at the start of the flow path. For the term $R$ the following equation can be derived:

$$R = \int_0^L \frac{1}{h^3}\,dx = \frac{L(\lambda+2)}{2\cdot h_s^3\cdot(\lambda+1)^3} \tag{4}$$

in which $\lambda$ is defined as the taper ratio:

$$\lambda = \frac{\Delta h}{h_s} \qquad (\lambda \geq -1) \tag{5}$$

For a parallel gap having $\Delta h = 0$ the taper ratio $\lambda = 0$. The resistance parameter $R$ can than be rewritten to:

$$R_{par} = \frac{L(0+2)}{2\cdot h_s^3\cdot(0+1)^3} = \frac{L}{h_s^3} \tag{6}$$

Substituting Eq. 6 in Eq. 3 gives the familiar equation of the leakage flow of a parallel gap:

$$Q_{par} = \frac{h^3\cdot b\cdot p_0}{12\cdot L\cdot\eta} \tag{7}$$

The ratio between the leakage flow of a tapered gap and the leakage of a parallel gap can now be described as a sole function of the $\lambda$-ratio:

$$\frac{Q}{Q_{par}} = \frac{2\cdot(\lambda+1)^2}{\lambda+2} \tag{8}$$

Equation (3) can be rewritten to define the local pressure $p(x)$ in the leakage gap:

$$p(x) = p_0 - \frac{12\cdot\eta\cdot Q}{b}\int_0^x \frac{1}{h^3}\,dx \tag{9}$$

Substituting the equations above for $h$ and $Q$, and applying the definition of $\lambda$ (Eq. 5), the pressure profile in the gap can be described as follows:

$$p(x) = \frac{\left([L-x]\left[L\{\lambda+2\}+\lambda\cdot x\right]\right)}{(\lambda+2)(L+\lambda\cdot x)^2}\cdot p_0 \tag{10}$$

The calculated pressure profile can be seen in the diagram below which shows the non-dimensional position $x/L$ in the gap on the horizontal axis and the pressure ratio $p(x)/p_0$ on the vertical axis for different values of the taper ratio $\lambda$. The parallel gap ($\lambda = 0$) has the familiar linear pressure profile. Converging gaps ($-1 \leq \lambda < 0$) cause an increase of the local gap pressure whereas for diverging gaps ($\lambda > 0$) the local pressure is decreased.

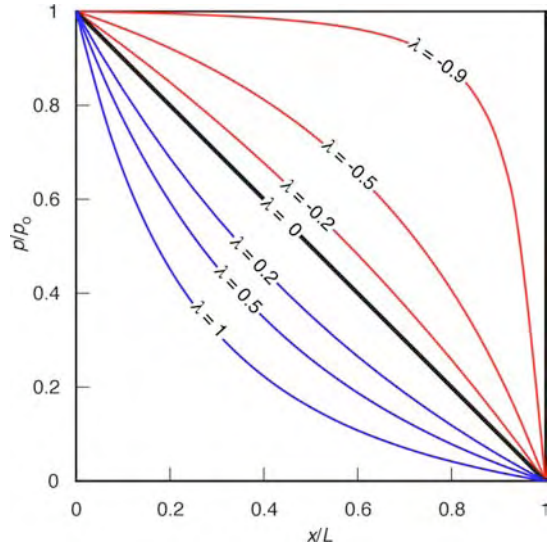


**Fig 10: Pressure profile in a sealing gap for different taper ratios $\lambda$.**

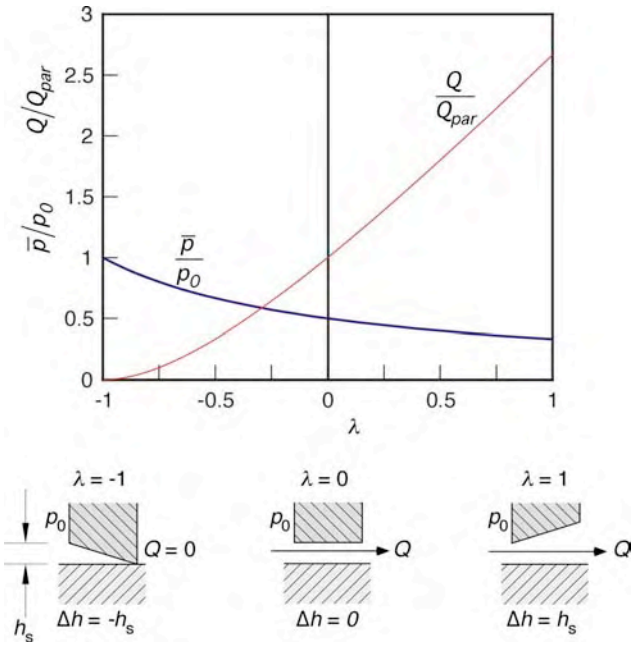


**Fig 11: Influence of the taper ratio $\lambda$ on the mean pressure in the gap and the leakage flow via the gap**

Equation 10 can be used to calculate the average pressure across the leakage gap, which determines in the end the load carrying capacity of the mechanical face seal:

$$\bar{p} = p_0 \frac{1}{\lambda + 2} \tag{11}$$

or

$$\frac{\bar{p}}{p_0} = \frac{1}{\lambda + 2} \tag{12}$$

Similar equations as shown before have previously been derived for mechanical face seals [3, 4] as well as for radial slipper bearings [15]. The dimensionless ratios presented in Eq. 8 and 12 are depicted in Figure 11. For a parallel gap, the mean pressure in the gap is half the pressure level at the gap entrance, which fits the familiar linear pressure profile in the gap. If the gap is tapered, the mean pressure can be doubled (in case of a converging gap, totally closing the gap at the end of the leakage path) or more than halved in case of a strongly diverging gap. It is also obvious that the gap profile has a significant influence on the leakage flow via the gap.

It is important to notice that the load carrying capacity of a hydrostatic thrust bearing i.e. of a barrel on a port plate is determined by a force differential (see Figure 17):

- the hydrostatic force $F_{cyl}$ pushing the barrel towards the port plate,
- the hydrostatic force $F_{seal}$ generated in the face seal pushing the barrel away from the port plate

If for instance $F_{seal} = 0.9\ F_{cyl}$ than a taper ratio of $\lambda = 0.22$ doubles the differential force $\Delta F = F_{cyl} - F_{seal}$. Hence a small variation of the taper ratio $\lambda$ can already significantly influence the remaining hydrostatic balance force.

## THE EFFECTS OF TAPERED DEFORMATION

The results of the FEM-analysis (Figure 8) and the calculated effects of the taper ratio on the mean gap pressure (Eq. 11) can now be used to calculate the hydrostatic force caused by the tapered gap. The extra force $F_{tap}$ created by the tapered gap relative to the parallel gap ($\lambda = 0$) can be defined as:

$$F_{tap} = A\left(\bar{p}_{tap} - \bar{p}_{par}\right) = A \cdot p_0 \left(\frac{1}{\lambda + 2} - 0.5\right) \tag{13}$$

in which $A$ is the area of the seal land and $p_0$ the pressure at the entrance of the gap (i.e. the pump pressure). Since $\lambda$ is defined as the ratio between the change of gap height relative to the initial gap height (Eq. 5) the taper value will change if the initial gap height is change. Because of this, the extra hydrostatic force $F_{tap}$ created by the tapered seal land will also change if the overall gap height between the barrel and the port plate is changed. Moreover, tilting positions of the barrel will cause a variation of the gap height and therefore result in a variation of $F_{tap}$ across the perimeter of the seal land.

The FEA-results presented in figures 2 and further are based on a calculation in which the components are assumed to make contact. In reality the barrel will at least to some extend be lifted or tilted from the port plate during operation. Assuming an extra gap height $h_0$ of 3 µm of the entire barrel (see Figure 15a), the taper ratio can be calculated. The results

are presented in the diagram of Figure 12. As can be seen, the gap has only a modest tapered shape being convergent for the most part of both seal lands. The taper ratio varies between $-0.24 < \lambda < 0.025$.

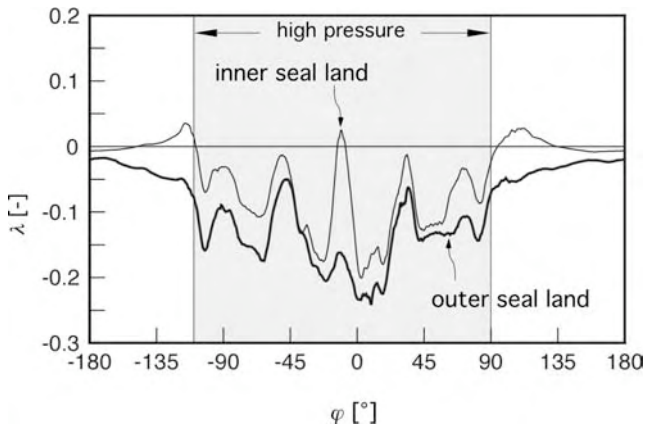


**Fig. 12: Taper ratio $\lambda$ for a 45 cc/rev slipper type pump at a pressure of 35 MPa, having an overall barrel lift of 3 µm.**

The slipper type machine, for which this calculation has been made, has an area of the inner seal land of 320.2 mm$^2$ and of the outer seal land of 416.5 mm$^2$. Dividing these seal lands in segments with an angular dimension of 0.5°, the extra hydrostatic force $F_{tap}$ can be calculated for each segment (Figure 13). The pressure increase that is caused by the tapered profile of the gap is modest: on average the tapered gap creates a pressure increase in the gap of about 4%. This means that, for a first indication of the effects of the tapered gap profile, it is not necessary to recalculate the deformation of the bearing components.

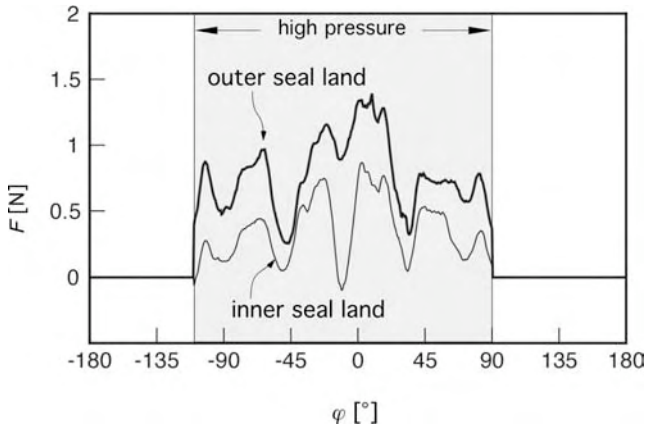


**Fig. 13: Extra hydrostatic force $F_{tap}$ per seal land segment of 0.5° at a pressure of 35 Mpa**

From these results the total extra lift force generated by the tapered gap can be calculated:

| | |
|---|---|
| Inner seal land: | $F_{tap}$ = 142 N |
| Outer seal land: | $F_{tap}$ = 311 N |
| Total: | $F_{tap}$ = 453 N |

As mentioned before the effects of the tapered gap are strongly dependent on the extra distance $h_0$ lifting the barrel as a whole from the port plate. Figure 14 shows the dependency of the total extra hydrostatic force $F_{tap}$ of both seal lands together for different values of the distance $h_0$. Even without changing the deformation of the barrel and the port plate, the taper ratio $\lambda$ will become larger if the barrel runs closer to the port plate. As a result the hydrostatic lift force acting on the barrel increases if the barrel approaches the port plate.

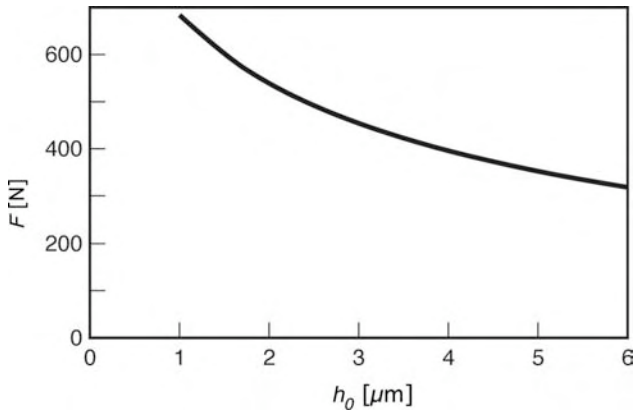


**Fig. 14: Influence of the extra gap height $h_0$ on the extra hydrostatic lift force $F_{tap}$ acting on the barrel (35 Mpa)**

## BARREL TILTING

Aside from an overall change of the barrel position the barrel can also have a tilted position. Starting with an initial gap height $h_o$ of 3 µm two situations will be examined:

- The barrel is tipped towards one of the dead centre positions on the port plate, reducing the gap height at this position with 2 µm to 1 µm and thus increasing the gap height equally at the opposite site (Figure 15b).
- The barrel is tipped towards the middle of the high-pressure port, also reducing the local gap height to 1 µm (Figure 15c).

Similar to the results presented in Figure 13, the extra hydrostatic force due to tilting can be calculated per seal land segment of 0.5°. The results are presented in the diagram of Figure 16. Instead of showing the separate forces for the inner and the outer seal lands, the two forces are added up in this diagram.

Tilting the barrel around the *x*-axis, for instance to the tilted position A, has almost no effect on the total $F_{tap}$. The reduced barrel height on one site on the barrel does indeed result in an increased local force due to the tapered gap profile, but on the other site across the barrel, the height is increased and the local $F_{tap}$ is decreased. The tilted position B however has a strong effect on $F_{tap}$, especially around the middle of the high-pressure port of the valve plate. The total value of $F_{tap}$ is now increased from 453 N for the parallel position to 637 N. This large influence is largely due to the local deformation of the housing, which causes the gap height at this location to be minimal. By tilting the barrel towards this bump in the valve

plate deformation (see Figure 6) the local gap height becomes very small and, as a result, the local $F_{tap}$ increases strongly.

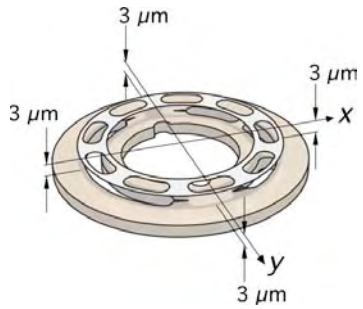


**15a. Parallel position $h_0$ = 3 μm**

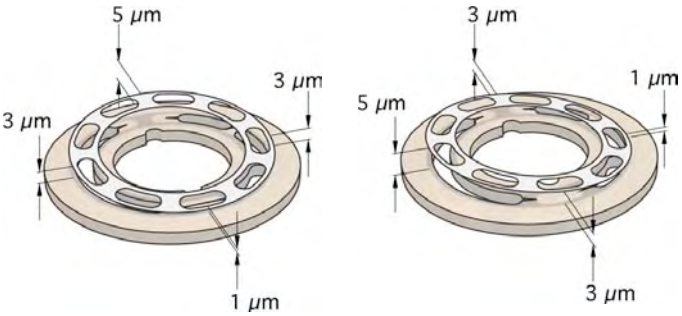


**15b. Tilted position A** **15c. Tilted position B**

**Fig. 15: Barrel positions**

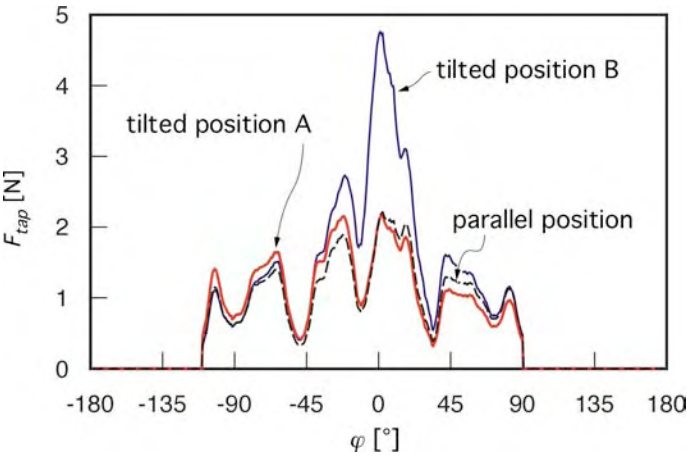


**Fig. 16: The effect of a tilted barrel position on the local $F_{tap}$ per seal land segment of 0.5° (35 MPa)**

The increased local taper effect around the $\varphi = 0°$ position (Figure 16) not only enlarges the extra lift force on the barrel but also creates a torque around the *y*-axis which counteracts the tilting of the barrel. Apparently the tapered gap stabilizes the barrel position in this direction. However, tilting the barrel in the opposite direction –around the *x*-axis– the tapered seal lands hardly have any effect due to the large deformations of the housing (as was described before). This emphasizes the importance of including the deformation of the housing in calculating the forces and moments created by the oil film between the barrel and the port plate.

## EFFECTS ON TORQUE LOSSES

The gap height depends on the forces and moments acting on the barrel. Ignoring the inertia forces, the force balance can be simplified to:

$$F_{sp} + F_{cyl} - F_{seal} = F_{contact} \tag{14}$$

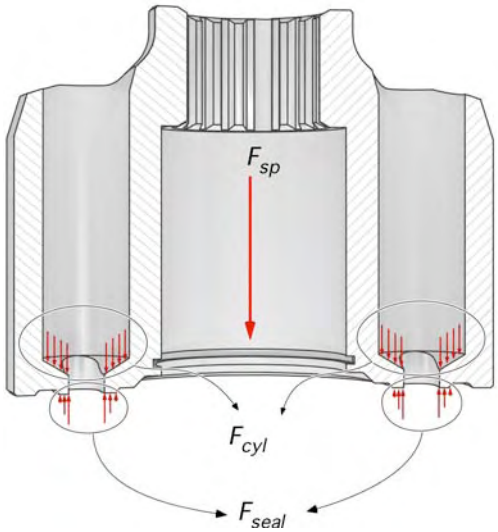


**Fig.17: Cross section of the barrel of a slipper type pump**

Neglecting the hydrodynamic forces in the oil film, the hydrostatic force caused by the oil film can be split in a force that would have been caused by a parallel gap, and an extra force resulting from the tapered gap profile:

$$F_{seal} = F_{par} + F_{tap} \tag{15}$$

The barrel can be dimensioned as such that the barrel is hydrostatically balanced, assuming a parallel gap profile:

$$F_{cyl} = F_{par} \tag{16}$$

Assuming the barrel is lifted from the port plate, the contact force $F_{contact} = 0$. As a result Eq. 14 can be reduced to:

$$F_{sp} = F_{tap} \tag{17}$$

Earlier it was already shown that the lift force created by the tapered gap is dependent on the distance between the barrel and the port plate (see Figure 15). According to Eq. 17, the barrel will be lifted to a position at which the lift force from the tapered field is counteracted by the force $F_{sp}$ of the barrel spring. The pump pressure has a direct influence on the lift force $F_{tap}$, also because the pressure influences the deformation and hence the taper ratio $\lambda$. The pump pressure also affects the general deformation of the pump components, resulting in a larger average gap height at higher pump pressures.

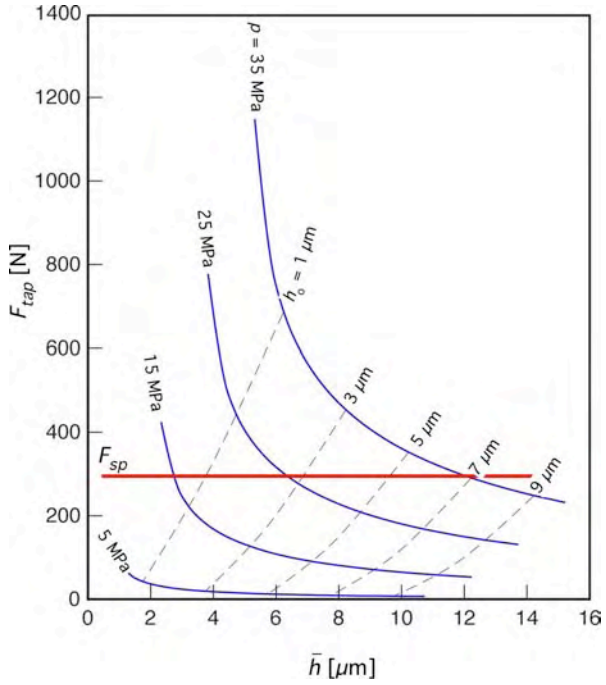


**Fig. 18: Influence of the pump pressure on the lift force $F_{tap}$ and the average gap height $\bar{h}$ for different values of the initial gap height $h_0$**

The effects of the pump pressure on the lift force $F_{tap}$ and the average gap height can be calculated by means of the results of the FEM-analysis. Both the lift force and the average gap height are also dependent on the initial gap height $h_0$. The calculated results of the variation of the pressure and the initial gap height are presented in Figure 18, showing the average gap height on the horizontal axis and the extra hydrostatic force generated by the tapered gap on the vertical axis. Also indicated in Figure 18 is a value for the barrel spring force. The point where, for a certain pressure level, the $F_{tap}$-line crosses the horizontal line of the spring force $F_{sp}$ indicates the average gap height for this condition.

The above analysis assumes only a barrel displacement in the axial *z*-direction. In reality the barrel is also free to turn around the *x*- and *y*-axis, as indicated in Figure 15. For this reason, aside from the axial force balance considered above, the torque balances around these axes have to be considered as well. In most cases the forces pushing the barrel towards the port plate ($F_{sp}$ and $F_{cyl}$) will not be in line with the forces acting on the seal lands of the barrel. The resulting torque will tip the barrel until the torque and force balance is restored again. This could well result in a contact force between the barrel and the port plate. In the end, the torque loss $M_{bf}$ created by the rotating barrel is equal to the sum of the coulomb friction torque $M_{cf}$ caused by the contact force and the viscous drag moment $M_{vf}$ of the remaining oil film:

$$M_{bf} = M_{cf} + M_{vf} = F_{cont} \cdot \mu \cdot r + M_{vf} \qquad (18)$$

If again the condition of Eq. 16 is fulfilled than Eq. 14 can be rewritten to:

$$F_{contact} = F_{sp} - F_{tap} \qquad (19)$$

For a given pump design, the spring force $F_{sp}$ is a constant. $F_{tap}$ on the other hand is dependent of the pump pressure but independent of the rotational speed, assuming dynamic buffer effects can be neglected. Hence $M_{cf}$ will not be influenced by the rotational speed of the pump. Conversely the rotational speed does have an influence on the other torque loss, $M_{vf}$ :

$$M_{vf} = c_{vf} \cdot n \cdot \iint \frac{1}{h(\varphi, r)} d\varphi \, dr \qquad (20)$$

The viscous drag is also influenced by the pump pressure, since the pressure level directly and indirectly influences the gap height *h*:

- A higher pressure creates a larger, overall elastic deformation of the pump components and therefore an increased gap height;
- A higher pump pressure increases the local deformation of the seal lands, which could cause an increased tapered gap effect, pushing the barrel away from the port plate.

## EXPERIMENTAL VALIDATION

It is not yet possible to calculate the complicated force and torque balance of the barrel, including the elastic deformation of all relevant pump parts and the effects of the tapered seal lands. It even becomes more complicated if buffer and squeeze effects have to be included. Eventually even wear and thermal effects must be taken into account in order to calculate all relevant effects of deformation on the load carrying capacity of the barrel seal lands.

But also an experimental verification of the effects of tapered sealing gaps on the load carrying capacity of a barrel in axial piston pumps or motors is no sinecure. The FEM-analysis has clearly shown that the deformation of the housing has a significant effect on the sealing gap behavior. It is therefore not just possible to isolate the port plate and the rotating group, thereby creating the possibility to get a better access to the rotating parts and gain more space for sensors. Measuring the barrel position by means of three position sensors also does not provide sufficient information since it is not known which part of the measured gap height is due to the local barrel movement and which part is due to the local deformation of the barrel and the housing.

A different approach is to measure the torque losses between the barrel and the port plate, since these losses are strongly influenced by the gap profile, as was proven in the previous paragraph. The floating cup pump (Figure 19, [23…29]) seems to be an ideal apparatus for this test.

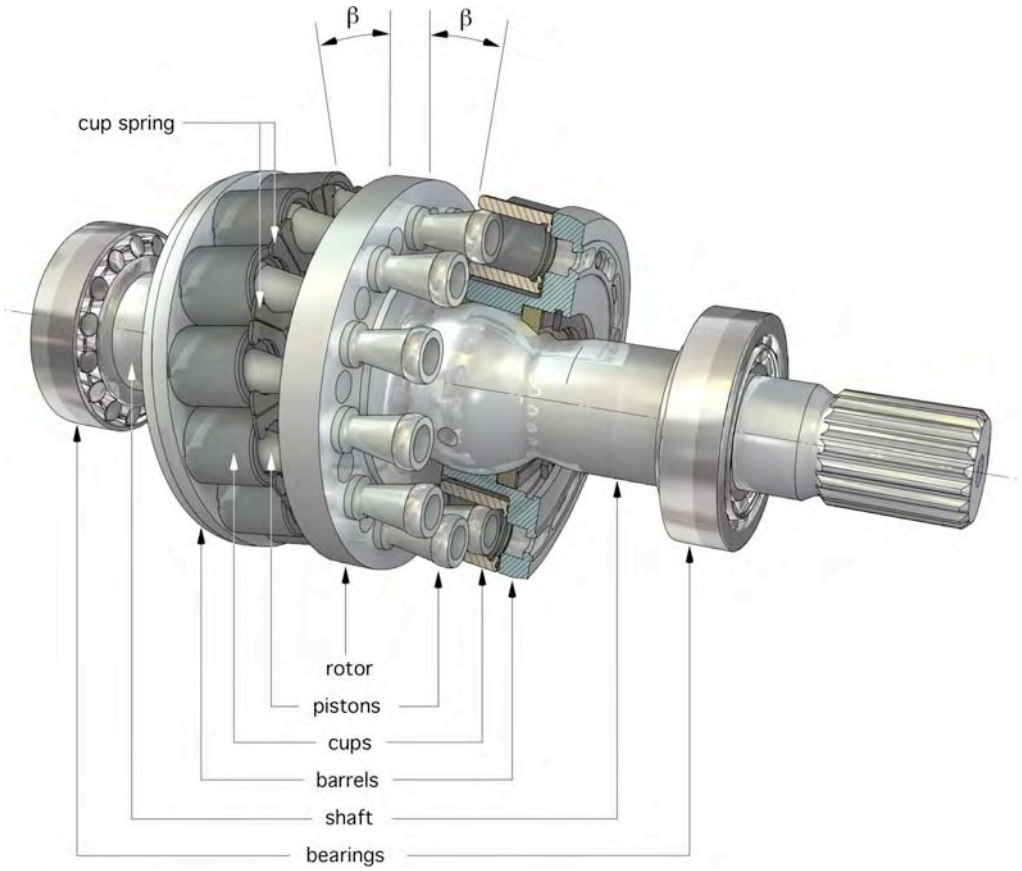


Main characteristics:

- Displacement (fixed): V = 28.2 cc/rev
- 24 pistons
- tilt angle of the barrel: $\beta = 8°$
- radius pitch circle pistons: $r_p = 36$ mm
- seal lands: $\Delta r = 1.4$ mm
- barrel material: brass (CuSn8, E-modulus = 114 GPa)
- port plate material: steel (E-modulus = 194 GPa)
- force barrel spring $F_{sp} = 240$ N

**Fig. 19: rotation group and main characteristics of the floating cup pump**

In most axial piston pumps and motors the viscous friction between the barrel and the port plate is only one of the many sources of torque losses. Other important sources are the pistons (and the eventual piston rings) the piston slippers and the roller bearings. In the axial piston, floating cup principle however, most friction losses of the floating cup principle are very small:

- There are no piston rings. Instead the cylinder seals directly on the ball shaped piston crown.
- The separated, floating cylinders are hydrostatically balanced. Therefore there is almost no contact force between the cylinder and its piston.

Due to the low relative velocity and a balanced cup construction the friction losses between the cups and the barrel plate are negligible. Conversely the pump has a double, mirrored construction with two sets of a barrel (plate) and a port plate. Also, the barrels have a relatively large pitch circle of the ports, which results in large seal lands and high relative velocities. As a result the torque losses of a floating cup pump are largely dominated by the viscous drag between the barrels and their port plates.

Figure 20 shows the torque loss based on measurements performed by the Technical University of Eindhoven in the Netherlands [30]. The diagram shows the total torque loss of a 28 cc floating cup pump as a function of the rotational speed and the pump pressure. As could have been expected the torque loss increases linearly with the speed, due to viscous drag (see Eq. 20).

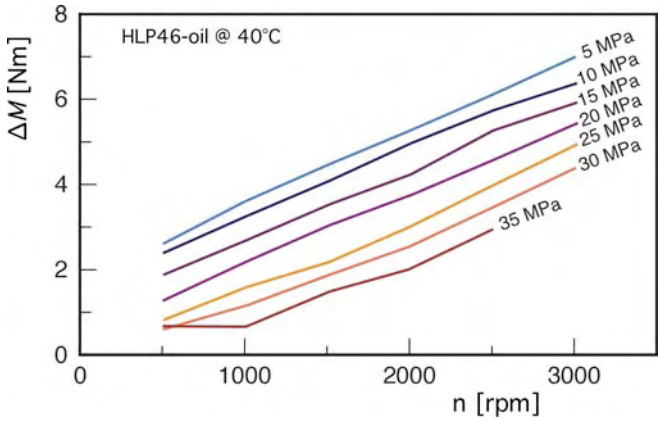


**Fig. 20: Total measured torque loss of a floating cup pump (28 cc/rev) as a function of the rotational speed and the pump pressure.**

Furthermore the torque loss is clearly dependent on the pump pressure: an increased pressure level reduces the torque loss. This could be explained by the effect of the tapered deformation of the seal lands. The pump has been designed as such that, assuming parallel seal lands, the barrel is hydrostatically balanced (Eq. 16). This means that effectively the barrel is pushed to the port plate by means of the barrel spring. Figure 21 shows the calculated resulting axial force $F_z$

and moments around the *x*- and *y*-axis of the barrel for a pump pressure of 35 MPa, as a function of the rotative position of the barrel. The *x*- and *y*-axes are defined as in figure 15a.

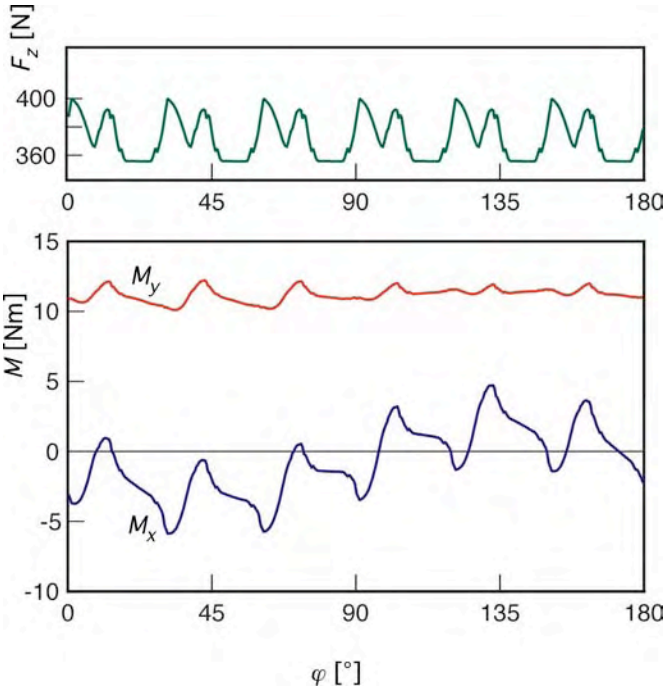


**Fig. 21: Calculated resulting axial force $F_z$ and moments $M_x$ and $M_y$ on a barrel of a floating cup pump, assuming parallel gaps, at a pump pressure of 35 MPa.**

The tapered seal lands create an extra hydrostatic axial force. Whereas the resulting force $F_z$ calculated for the parallel gaps pushes the barrel down towards the port plate, the hydrostatic force created by the tapered seal lands pushes the barrel upwards, away from the port plate. Since the taper force becomes smaller when the gap height is increased the barrel will find a force and torque balance at a tilted position. Thereby the barrel could well make contact with the port plate. Similar metal-to-metal contacts are also observed with other hydrostatic trust bearings [17].

Raising the pump pressure results in an increased deformation of the barrel and a stronger tapered shape of the sealing gaps. This reduces the contact force between the barrel and the port plate (see Eq. 19). Consequently the coulomb friction and the total torque loss are reduced as well (Eq. 18). Because the coulomb friction is not dependent on the rotational speed the lines in Figure 20 are all parallel, till a pressure level (at 35 Mpa) at which the barrel is lifted completely from the port plate and the torque losses are foremost dominated by other losses.

## THE DEVIL IS IN THE DETAIL

The tapered deformation of the seal lands could well explain the experimental results measured on the floating cup pump, but it doesn't give experimental evidence. Research in the field of mechanical face seals has also proven that waviness of the seal lands (in the axial direction) can also create a substantial hydrodynamic effect. The deformation of both barrel and port plate also shows tangential deformations that could cause an extra hydrodynamic force that could also contribute to a pressure dependent reduced torque loss as shown in figure 20.

It is also evident that the pressure profile in the sealing gap will effect the deformation. This will again change the pressure profile in the gap. Dynamic buffer effects will also have a substantial influence on the pressure profile and hence on the deformation. In order to describe these phenomena an extensive EHD-model of the main components is needed. As was shown in this paper it is also necessary to include at least part of the housing of the pump in this model. In the end, small local deformations across the sealing gap, being one micrometer or even less, can well create forces on the barrel that are in the same order as the remaining hydrostatic balance force or the force of the barrel spring.

## REFERENCES


[1] Lebeck, A.O., 1991, Principles and design of mechanical face seals, John Wiley & Sons, ISBN 0471-51533-7

[2] Pascovici, M.D., Etsion, I., 1992, A thermo-hydrodynamic analysis of a mechanical face seal, Journal of Tribology, Oct.1992, Vol. 114, pp.639-645

[3] Cicone, T., Pascovici, M.D., Tournerie, B., 2001, Non-isothermal performance characteristics of fluid-film mechanical face seals, Proc Instn Mech Engrs Vol 215 Part J, pp. 35-44

[4] Lubbinge, H., 1999, On the lubrication of mechanical face seals, Thesis University of Twente, ISBN 90-3651240-9

[5] Dadouche, A., Fillon, 2000, Analyse théorique et expérimentale des effets thermiques dans les butées hydrodynamiques à géométrie fixe, Mec. Ind., 1, pp. 141-150

[6] Brunetière, N., Tournerie, B., Frêne, J., (2003), A simple and easy-to use TEHD model for non-contacting liquid face seals, Tribology Transactions, Vol 46, 2, pp 187-192

[7] Brunetière, N., Tournerie, B., Frêne, J., (2003), TEHD Lubrication of mechanical face seals in stable tracking mode: Part 1 – Numerical Model and experiments, Transactions of the ASME, Vol. 125, pp. 608-616

[8] Brunetière, N., Tournerie, B., Frêne, J., (2003), TEHD Lubrication of mechanical face seals in stable tracking mode: Part 2 – Parametric Study, Transactions of the ASME, Vol. 125, pp. 617-627

[9] T. Kazama, Yamaguchi, A., 1993, Optimum design of bearing and seal parts for hydraulic equipment, Wear, Vol 161 p. 161-171

[10] X. Wang, Yamaguchi, A., 1999, Characteristics of the bearing/seal parts of piston pumps and motors for water hydraulic systems, Proc. Forth JHPS International Symposium pp. 345-350

[11] Kazama, T., Yamaguchi, A., Fujiwara, M., 2002, Motion of eccentrically and dynamically loaded hydrostatic thrust bearings in mixed lubrication, Proc. 5th JFPS Int. Symposium, ISBN 4-931070-05-3, pp. 233-238.

[12] Huang, C., Ivantysynova, M., 2003, A new approach to predict the load carrying ability of the gap between valve plate and cylinder block, Power Transmission and Motion Control PTMC 2003, ISBN 1-860584-14-4, pp. 225 – 239

[13] Ivantysynova, M., Huang, C., 2002, Investigation of the gap flow in displacement machines considering elastohydrodynamic effect. Proc. 5th JFPS Int Symposium, pp. 219-229

[14] Ivantysynova, M., 2003, Prediction of pump and motor performance by computer simulation, 1st Int. Conf. on Computational Methods in Fluid Power Technology, Melbourne November 2003, Australia, pp. 505 – 522

[15] Manring, N.D., Johnson, R.E., Cherukuri, H.P., 2002, The impact of linear deformations on stationary hydrostatic thrust bearings, Transactions of the ASME, Vol. 124, pp. 874-877

[16] Manring, N.D., Wray, C.L., Dong, Zhilin, 2004, Experimental studies on the performance of slipper bearings within axial-piston pumps, Journal of tribology, July 2004, Vol. 126, pp. 511-518

[17] Crabtree, A.B., Manring, N.D., Hohnson, R.E., 2005, Pressure measurements for translating hydrostatic thrust bearings, Int. Journal of Fluid Power, Vol. 6, nr. 3

[18] Winkler, B., Hametner, G., Scheidl, R., Manhartsgruber, B., Modeling and simulation of the elasto-hydrodynamic behavior of sealing gaps, 1st Int. Conf. on Computational Method in Fluid Power Technology, Melbourne Australia

[19] Kojima, E., Yamazaki, T., 2003, Prediction of sound power radiated from oil hydraulic pump by FEM and BEM, PTMC 2003, 10-12 September/ University of Bath, p. 265

[20] Müller, B, 2002, Einsatz der Simulation zur Pulsations- und Geräuschminderung hydraulischer Anlagen, IFAS Reihe Fluidtechnik, Band 82, Thesis RWTH Aachen University

[21] Kudav G., Kasper, L., Zhang, H., Kimpel, R., 2005, Development of a heavy duty piston pump using flexible body approach, NCFP I05-10.3, Proc. 50th National Conf on Fluid Power, IFPE 2005, Las Vegas, pp. 349-359

[22] Kunze, T., Berneke, S., 2006, Noise reduction at hydrostatic pumps by structure optimization and acoustic simulation, proc 5th IFK, Aachen

[23] Achten, P.A.J., 2002. "Dedicated design of the Hydraulic Transformer", Proc. IFK.3, Vol. 2, IFAS Aachen, pp. 233-248

[24] Achten, P.A.J., van den Brink, T.L., Potma, J.W., 2004, "Movement of the cups on the barrel plate of a floating cup, axial piston machine", International Journal of Fluid Power, 5(2)

[25] Vael, G.E.M., López Arteaga, I., Achten, P.A.J., 2004, "Reducing Flow Pulsations with the Floating Cup Pump: Theoretical Analysis", Proc. PTMC 2004, Bath

[26] Achten, P., van den Brink, T., Schellekens M., Design of a variable displacement floating cup pump, Proc. 9th Scandinavian Int. Conf. on Fluid Power, SICFP'05, Linköping, Sweden.

[27] Achten, P.A.J., 2005, Volumetric Losses of a Multi Piston Floating Cup Pump, NFPA/IFPE 2005, Las Vegas, March 16-18, 2005

[28] Achten, P.A.J., 2004, Power Density of the Floating Cup Axial Piston Principle, IMECE2004-59006, 2004 ASME Int. Mech. Eng. Congress and Exposition, November 13-20, 2004, Anaheim, California USA

[29] Achten, P.A.J., Schellekens, M., Murrenhoff, H., Deeken, M., 2004, Efficiency and Low Speed Behavior of the Floating Cup Pump, SAE 2004-01-2653

[30] Post, W., 2004, Determination of steady-state performance of Innas Floating Cup type of axial piston pumps (ISO 4409), DCT-report 2004-127, Eindhoven Technical University

## APPENDIX A: THERMAL EFFECTS ON THE OIL VISCOSITY

In the above analysis the leakage flow is assumed to be isoviscous and isothermal. Yet, the energy dissipation effect of throttling and viscous friction will cause heat generation in the oil film. As a consequence the oil temperature will rise and the viscosity will be reduced. On the other hand the barrel and the port plate will cool down the thin oil film in the narrow gap. In the end the question is not if the oil temperature will rise, but if the resulting change of oil viscosity will have such an effect on the performance of the face seal between the barrel and the port plate that it cannot be neglected in the calculations.

There is almost no previous research about temperature effects of the oil film between barrels and port plates. Ivantysynova [12, 13] has emphasized the importance of the viscosity change in the numerical modeling of the seal land gap. Other researchers just neglected the change of temperature and viscosity [9, 10, 11, 15, 18] and assumed an isothermal, isoviscous flow.

More research has been performed on face seals in other applications than hydrostatic machines [1…8]. But also these publications do not give much information about the heat balance, heat transfer coefficients or Nusselt or Prandtl numbers of the thin oil film. It is also questionable whether these research results can be applied to face seals in pumps and motors. There are at least some important differences to be considered:

- The pressure levels in hydrostatic pumps and motors are much higher than in general face seal applications outside hydrostatic machines
- The mechanical face seal components in pumps and motors are much better cooled due to the surrounding oil and the high flow of the pumped oil that acts as a cooling medium.
- Seal lands in hydrostatic pumps and motors are generally shorter (in the radial direction of the leakage flow). Consequently the viscous losses will be lower than in face seals applied outside pumps and motors.
- The higher pressure levels increase the throttle losses.

Consequently face seals are to a lesser extend or even not all deformed by the pressure load. Conversely they are much more prone to thermal loads causing thermal expansion of the mechanical components of the face seal. The necessity of thermoelastohydrodynamic (TEHD) analysis of mechanical face seals is because of these deformations (which cause the sealing gap to become tapered), not because of the influence of the heat balance on the viscosity.

The question remains if, and to what extend the heat balance of the oil film between the barrel and the port plate will substantially influence the performance of the seal. Instead of calculating the heat balance itself, Cicone et al [3] have calculated the effects of a possible viscosity change on the bearing performance. The theoretical approach is similar to the analysis described in the previous paragraph, only now a linear temperature increase in the gap has been assumed. The conclusion of this analysis is that, for a practical range of seal operation conditions, the accuracy of the isoviscous solution is acceptable for calculation of the load carrying capacity, the film stiffness and the frictional torque. Only for the calculation of the leakage flow rate the temperature increase of the oil can have a more significant influence.




© 2006 by Innas BV, The Netherlands